Journal of Solid State Chemistry **156,** 154–160 (2001)
doi:10.1006/jssc.2000.8975, available online at http://www.idealibrary.com on IDEAL®

Modeling Ionic Conductivity in Nasicon Structures

Daniele Mazza

Dipartimento di Scienza dei Materiali e Ingegneria Chimica, Politecnico di Torino, Corso Duca degli Abruzzi 24, 10129 Torino, Italy

Received May 30, 2000; in revised form August 23, 2000; accepted October 3, 2000; published online January 3, 2001

Considering only the structure of oxygen lattice and employing bond valence equations, the conduction geometry and the activation energy of Na^+ motion in Nasicons are modeled. This is performed by calculating the valence sum $m(x, y, z)$ for a grid of points inside the oxygen lattice, then by following with iterative procedures the pathway with lowest relative $m(x, y, z)$ values, starting from a specified position and initial direction. After a certain trajectory the Na^+ ion will reach a second position in the lattice, which will usually correspond to a known crystallographic position. Different rhombohedral and monoclinic Nasicons are examined, enabling us to verify some the ionic movement. Structural parameters governing conduction are described, based on the distortions of real structures from an idealized (archetype) Nasicon structure, in turn modeled by bond valence equations. © 2001 Academic Press

Key Words: **Nasicon; bond valence; sodium ion; ionic conductivity; activation energy.**

INTRODUCTION

Since Hong and Goodenough *et al.* (1,2) discovered Nasicon (Na superionic conductor) materials, great interest has been devoted by many researches to investigating the properties of structure, crystal chemistry, and fast ionic conductivity. The three-dimensional framework of such a structure is constituted by robust connection of ZrO_6 octahedra and $(Si, P)O_4$ tetrahedra sharing corner oxygens. Every two octahedra there are three tetrahedra present. This framework generates in its interior the conductive pathways responsible for the superior Na^+ mobility. The complete substitution of P for Si in the tetrahedral sites allows the formation of a solid solution series. This is expressed by the well known notation $Na_{(1+x)}Zr_2Si_{(x)}P_{(3-x)}O_{12}$ with $0 \le x \le 3$. The symmetry of the different terms is rhombohedral (s.g., $R\text{-}3c$) except for a certain range ($1.6 < x < 2.4$) where the samples display monoclinic symmetry (s.g., $C2/c$) at room temperature, with a transition to rhombohedral symmetry near 170°C (3). A second substitution mechanism, Na for Zr in the octahedral sites, was evidenced later (4, 5). This makes it possible to form a second mixed crystal series with stoichiometry $Na_3Zr_{(2-x/4)}Si_{(2-x)}P_{(1+x)}O_{12}$ ($0 < x < 1.67$) with rhombohedral symmetry, except for a short monoclinic range ($0 < x < 0.33$). This series shows constant Na content and the charge imbalance due to the Na–Zr substitution is compensated by a contemporary Si–P substitution on tetrahedral sites. Kohler *et al.* (6) examined the diffusion path in a high-temperature single crystal with composition close to the term of this series with $x \approx 0.75$. They pointed out that anisotropy and magnitude of the temperature factors are both extremely high and on this basis a joint probability density function was proposed to describe the conduction path.

Most authors agree that structural features are the key to explaining the conduction mechanism, but also the number of ionic carriers and their distribution over the different sites are factors likely affecting conductivity (7). Up to now, modeling Na site occupancies and Na^+ conduction mechanisms has been attempted by empirical correlation with structural factors. Some authors found correlation with unit-cell parameters a_0 and c_0, or with unit cell volume. More recently, other geometrical factors were scrutined, like the size of the bottlenecks which connect different Na sites in the structure (8) or the occupation of intermediate Na positions in the conduction channel (called mid-Na) (9).

The conduction pathway among the different Na positions of the rhombohedral Nasicon has been long debated. When TranQui *et al.*, (8) determined the crystal structure of $Na_4Zr_2Si_3O_{12}$ they proposed one conduction path between Na1 and Na2 and a second from Na2 to neighboring Na2. The latter was held more important because of the wider channel opening involved. Kohler *et al.*, in their investigation (6) on a Zr-deficient composition ($Na_{3.1}Zr_{1.78}Si_{1.21}P_{1.76}O_{12}$) found the path from Na1 to Na2 be energetically more probable on the basis of the Fourier transform of temperature factors. Subramanian *et al.* investigated different scandium-substituted Nasicons and concluded that the Na2–Na2 pathway is more likely in the rhombohedral phase (10). Recently Losilla *et al.* (11) examined the series of Nasicons $Na_{1.4}M_{1.6}In_{0.4}PO_{12}$ (M = Ti, Sn, Hf, Zr) and evidenced that two bottlenecks affect the Na mobility from Na1 to Na2 positions, excluding direct connection between Na2 and Na2 positions.

0022-4596/01 $35.00

The lowest activation energies for ionic conduction are reported for the monoclinic phase ($x \approx 2$) (3), however, ionic pathways are still not defined and only inferred from similarity to the rhombohedral phase.

IDEALIZED NASICON STRUCTURE

Before modeling the conduction in different Nasicons, we wish to describe an idealized structure (archetype), and therein the conduction path will be evidenced. We show that real structures derive there from by small rotations/deformations of bonds, which in turn influence conduction paths and energy barriers for ionic movement.

The archetype structure consists of a close packed structure, in which all the distances between contacting oxygen ions are kept equal. Therefore we suppose that all oxygen ions are hard spheres with equal radius and then we construct idealized coordination polyhedra around Zr and (Si, P). As second step we arrange the polyhedra in the most symmetric and close-packed manner.

A Zr polyhedron can be easily modeled as a regular octahedron with two opposite faces parallel to the *ab* plane and having the three corner oxygens directed along [100], [010], [$\bar{1}\bar{1}0$] directions for one face and along [110], [$0\bar{1}0$], [$\bar{1}00$] directions for the opposite face (supposing hexagonal symmetry). Two Zr octahedra, rotated 60° one with respect to each other, are stacked along *c*, so that a triangular prism is formed between them. Inside this prism no cations are contained, but the three pairs of facing oxygens along *c* form two of the four corners of three (Si, P) tetrahedra. This block constitutes the asymmetric unit of the framework, as pointed out by many authors (1–4). It has the chemical composition $2 \cdot Zr(O)_6 + 3 \cdot (Si, P) = Zr_2\ (Si, P)_3 O_{12}$ with a number of negative charges (1 to 4) depending on the Si/P ratio. These building units are in turn stacked along *c*, being connected by Na1 counterions. These Na^+ ions result coordinated by six oxygen atoms, located at the vertices of a triangular antiprism. In this way an infinite ribbon is originated, as shown in Fig. 1., which derives from the sequence

$$\cdots\text{–}ZrO_6\text{–void–}ZrO_6(\text{rotated by } 60^\circ)\text{–Na1–}\cdots$$

If our idealized picture is described in the *R*-3*c* space group, it can be geometrically shown that coordination polyhedra are regular and all the contacting oxygen atoms are at the same distance (i.e., the O–O distance will be twice the O ionic radius, which is kept constant for all oxygen atoms in the structure) if O1 is placed at ($\frac{1}{6}$, 0, $\frac{1}{6} + \delta$) and O2 at ($\frac{1}{6}$, $\frac{1}{6}$, $\frac{1}{12}$). The δ parameter can be unambiguously determined if we consider that (in the *R*-3*c* space group) the infinite ribbons along *c* are shifted by symmetry by ($+\frac{1}{3}$, $+\frac{2}{3}$, $+\frac{2}{3}$) and ($+\frac{2}{3}$, $+\frac{1}{3}$, $+\frac{1}{3}$), and moreover by translation. The oxygen atoms of the primitive ribbon (0, 0, 0) must therefore

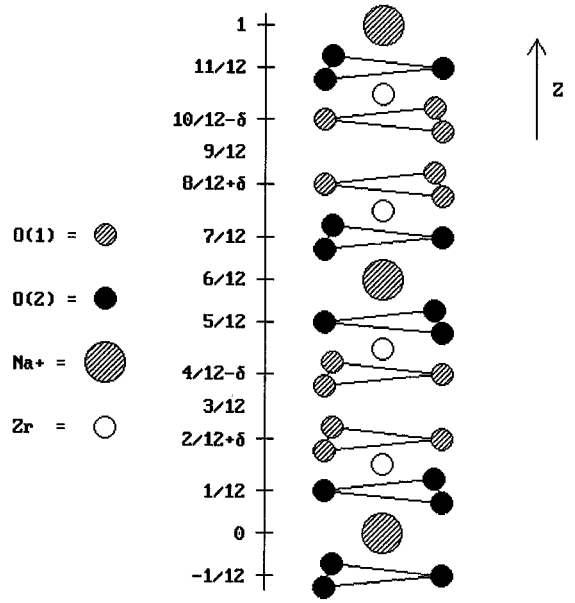

FIG. 1. Stacking of sodium and zirconium coordination polyhedra along *z* to form an infinite ribbon in the idealized model.

contact the oxygen atoms of the symmetry equivalent ribbons forming the regular coordination tetrahedra $(Si, P)O_4$. In our idealized model these tetrahedra must be constituted by four contacting hard spheres and therefore the tetrahedra become regular. This makes it possible to calculate the δ parameter and in turn the a_0, c_0 parameters of the idealized rhombohedral cell. If r_0 indicates the oxygen radius, one obtains

$$a_0 = 4 \cdot \sqrt{3} \cdot r_0,$$

$$c_0 = (4 \cdot \sqrt{2} \cdot \sqrt{3} + 6) \cdot r_0,$$

$$\delta = 2 \cdot (\sqrt{2}/(6 \cdot \sqrt{2} + 3 \cdot \sqrt{3}) - \tfrac{1}{6}) \cdot r_0 \approx 0.020 \cdot r_0.$$

Finally, the radius r_0 of the oxygen atoms can be predicted using bond valence equations (12–14), by minimizing at the same time the differences between the valence sum around any atom and its atomic valence (Valence Sum Rule) and the valence sum around any close loop in the bond graph (Equal Valence Rule).

The relating equations (13, 14, 16) are

$$s_{ij} = \exp[(R_0 - R_{ij})/0.37],$$

where $R_0(\text{Na}) = 1.803$, $R_0(\text{Si}) = 1.624$, $R_0(\text{P}) = 1.617$, $R_0(\text{Zr}) = 1.928$

$$V_i = \sum_j s_{ij},$$

$$0 = \sum_{\text{loop}} s_{ij}.$$

A least square refinement of both V_i and $\sum_{\text{loop}} s_{ij}$ yielded the result of $r_0 = 1.434$ Å, corresponding to a O–O distance of 2.867 Å that well compares to the mean value of O–O distances observed in Nasicons (e.g., 2.7990 Å, (9)). Na1 lies at the center of a regular oxygen octahedron, while Na2 lies at the center of an eightfold coordinated polyhedron.

Real structures are obtained by slightly rotating the opposite faces of the Na1, Zr coordination polyhedra of the archetype. In particular, referring to Fig. 1, the triangle built up by connecting three O(1) is rotated clockwise by an angle ε (between 4 and 9°) from its ideal position ($\varepsilon = 0$); this rotation will produce symmetry-equivalent rotations for all other O(1) triangles. The rotation of the second triangle, constituted by three O(2), is described by introducing a second angle ϕ which measures the relative rotation between O(1) and O(2) triangles. In the idealized model this angle ϕ equals 60° and in the real structure it is comprised between 57° and 63°. The effects of these slight rotations are fundamental to ionic mobility, as will be shown below. Because of the lack of an archetype model, up to now these effects have not been described in the literature.

VALENCE BOND ANALYSIS

This paper explores the use of bond valence equations (12–14) in order to predict the conduction geometry and mechanism both for monoclinic and rhombohedral Nasicons on the basis of the structural descriptions of oxygen lattice of the phase. Oxygen network carries a negative charge and contains interstices into which the mobile Na^+ cations are placed for charge balance. Bond valence rules are hence used to map the bond valence sum $m(x, y, z)$ that a Na^+ ion would have if placed on an arbitrary point (x, y, z) of these interstices (14). Points in this valence map corresponding to the valence of the ion (in this case 1) are energetically proper sites for it, a higher value representing a too small cavity, therefore with higher repulsive potential energy. Values smaller than one correspond to a large cavity, in which the ion has an anomalously high thermal factor. In these large interstices the sodium atoms have sufficient room and they are statistically distributed off-center within this space.

By moving the arbitrary point (x, y, z) over a grid covering the whole unit cell volume one can find the probable trajectory for the Na^+ ions. This can be done by following the points with lower $m(x, y, z)$ starting from a specified position (e.g., Na1) and following a certain initial direction (e.g., toward Na2). Then this direction is not fixed during the path, and the ion is left free to direct itself following the lowest $m(x, y, z)$ inside a solid angle with an iterative process. This simulates the effect of an external electrical force acting on the ion. After a certain trajectory, the ion quite easily reaches a second position in the lattice, which corresponds usually to a known crystallographic position for Na^+ ions. The valence sum for Na^+ ion can be plotted versus the distance (d) traveled along, thus obtaining a plot of $m(d)$ versus d(Å). Saddle points of the $m(d)$ function correspond to potential barrier (bottlenecks) encountered by the ion along its trajectory. The analysis of the $m(d)$ curves makes it possible to find the conduction hindrances (bottlenecks) to the ions movement for each Nasicon structure (where the O(1) and O(2) positions are known) and hence to relate this to the electrical characteristics of the materials.

For sake of clarity this treatment is divided in four parts, namely

(i) idealized Nasicon structure

(ii) rhombohedral Nasicons of the series $Na_{(1+x)}Zr_2Si_{(x)}P_{(3-x)}O_{12}$ $(0 \le x \le 3)$

(iii) miscellaneous Nasicons with rhombohedral symmetry

(iv) monoclinic Nasicon $Na_{(1+x)}Zr_2Si_{(x)}P_{(3-x)}O_{12}$ (with $x = 2.05$).

Idealized Nasicon Structure

Neighboring Na1–Na2 and Na2–Na2 distances are geometrically equal to 3.782 and 4.932 Å respectively; the real path traveled by the ion can be modeled by imposing that Na^+ ions follow the lowest $m(x, y, z)$ trajectory from the starting position to the arriving one (Na1–Na2 in Fig. 2a and Na2–Na2 in Fig. 2b). The corresponding $m(d)$ plots are shown in Fig. 3. The bottleneck for the trajectory Na1–Na2 corresponds to one face of the Na1 octahedron, while for the way Na2–Na2 this corresponds to the passage throughout a distorted triangle which builds one of the faces of the Na2 polyhedron.

If we compare the $m(d)$ maxima of the two trajectories (called hereinafter VUmax) one can conclude that the easiest path is unambiguously Na2–Na2.

Rhombohedral Nasicons of the Series $Na_{(1+x)}Zr_2Si_{(x)}P_{(3-x)}O_{12}$ (with $0 \le x \le 3$)

The sodium cations are located at different lattice positions, their total amount being determined by charge balance. In the rhombohedral phase Na^+ ions are place on two positions, namely Na1 and Na2, along the conduction channels. The variation in electrical conductivity along this series has been measured by many authors. A summary of these measurements has been reported elesewhere (7). The values were referred to 300°C, so as all compositions have rhombohedral symmetry (transition monoclinic to rhombohedral occurs at about 170°C for the range $2.00 \le x \le 2.25$). Taking into consideration the various terms with x varying from 0 to 3 in the solid solution, the $m(d)$ curves are calculated, both for the Na1–Na2 and for the Na2–Na2 path. Calculations show that the effects of the O(1), O(2) rotations from

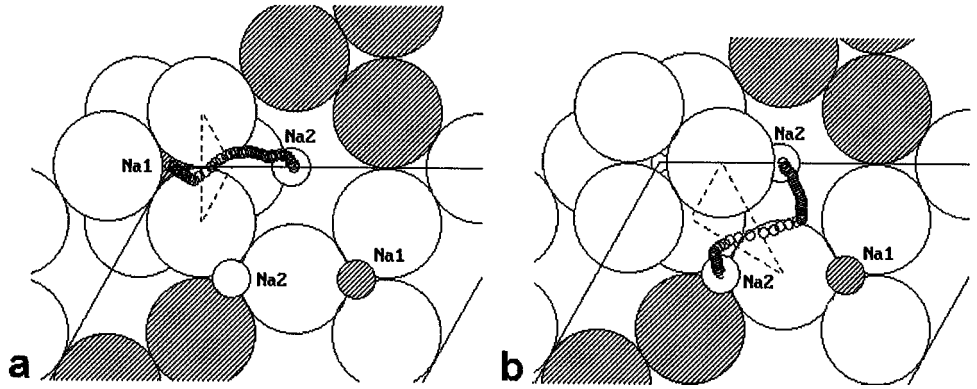

FIG. 2. (a and b). Projection onto the horizontal plane ($z = 0$) of the Na1–Na2 and Na2–Na2 conduction path in the idealized structure. The bottleneck triangle is drawn with dashed lines.

the idealized model are marked: by way of the rotation, the Na1–Na2 path becomes straighter, while simultaneously its saddle point decreases. On the contrary, the Na2–Na2 path changes its shape, however, remaining longer than Na1–Na2 (Fig. 4). It displays now two saddle points of nearly the same height with a depression in between. The Na2–Na2 path shows therefore two VUmax, very close to the VUmax of the Na1–Na2 path. By considering that the Na2–Na2 path is longer and displays two maxima, we can say that the Na1–Na2 path is more probable. The flex near $1.2 \approx 1.3$ Å along the conduction path Na1–Na2 corresponds to the mid-Na position pointed out by Boilot (9).

It is interesting to note that, although the shapes of the conduction paths Na1–Na2 and Na2–Na2 remain nearly unchanged, the height of the curves in terms of VU vary notably along the series as shown in Fig. 5. Two interesting correlations can be drawn. First between VUmax along the Na1–Na2 conduction path (values of the saddle points) and the logarithm of electrical conductivity (Ωcm at 300°C) and the second between the same VUmax and the two rotation angles ε and ϕ. Both relationships are linear, as shown in Fig. 6. This makes it possible to predict the conductivity on the basis of structural values only, in particular the two rotation angles. These angles seem to be the fundamental structural feature influencing the ionic conductivity along this series. It is noteworthy to remark that the term having $x = 2$ corresponds to the highest conductivity, and to the highest values of rotation angles ε and ϕ.

Miscellaneous Nasicons with Rhombohedral Symmetry

Substituted Nasicon compositions have been examined from the point of view of structure and ionic conduction.

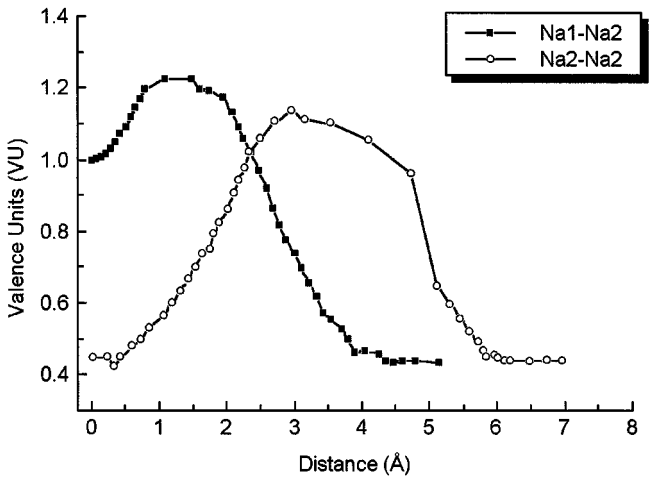

FIG. 3. $m(d)$ curves for Na1–Na2 and Na2–Na2 conduction path in idealized structure. The Na2–Na2 path has a lower VUmax value and the results are more probale.

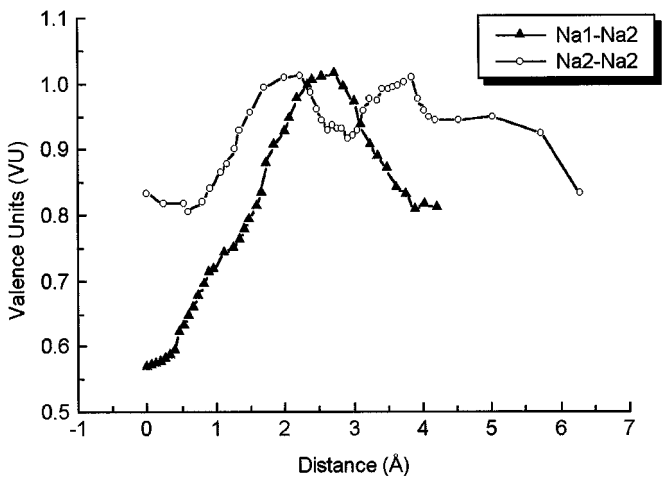

FIG. 4. $m(d)$ curves for Na1–Na2 and Na2–Na2 paths in rhombohedral $Na_{3.05}Zr_2P_{0.95}Si_{2.05}O_{12}$

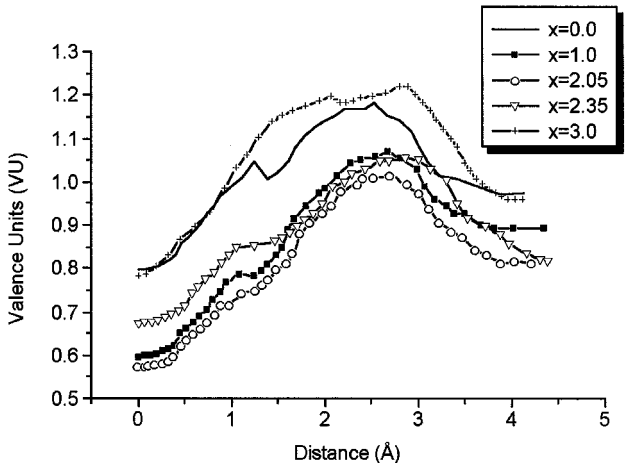

FIG. 5. $m(d)$ curves for Na1–Na2 paths for rhombohedral $Na_{(1+x)}Zr_2P_{(3-x)}Si_{(x)}O_{12}$ for different x values.

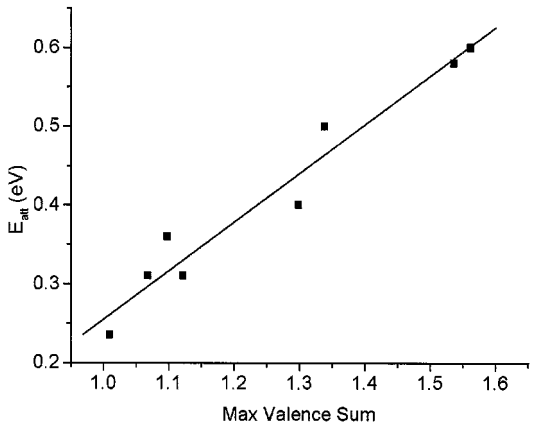

FIG. 7. E_{act} (eV) for ionic conduction versus VUmax for different substituted Nasicons.

Recently, rhombohedral compositions $Na_{1.5}Me_{1.5}In_{0.5}P_3O_{12}$ (Me = Ti, Sn, Hf, Zr) have been examined (11). Subramanian *et al.* examined substituted Nasicons, in which zirconium is substituted by scandium in the octahedral sites, the charge imbalance being compensated by substitution of Si by P substitution (10). On the basis of the reported structural data the Na1–Na2 path results are clearly more probable (Fig. 8); from the calculated trajectories the VUmax values are compared with the activation energies for ionic conduction which have been experimentally found for the same phases.

Fig. 7 shows a well interpolated linear relationship between these parameters for different substitutions. Moreover, the shape of the $m(d)$ curves (Fig. 8) for $Na_{1.5}Zr_{1.5}In_{0.5}P_3O_{12}$ confirms the two bottlenecks along the conduction path, as recently reported (11). The second bottleneck likely affects activation energy, as it can be estimated from its higher VUmax, in accordance with the results of Losilla *et al.* (11). The shape of $m(d)$ curves indicates that these

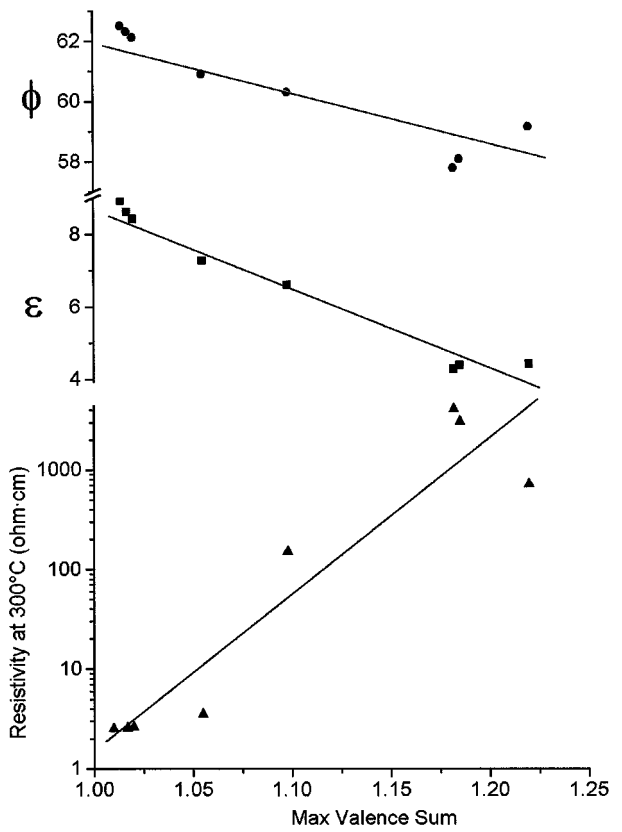

FIG. 6. Rotation angles in sexagesimal degrees ε (top), ϕ (center), and resistivity (bottom), versus VUmax for Nasicons of the rhombohedral series $Na_{(1+x)}Zr_2P_{(3-x)}Si_{(x)}O_{12}$. Linear interpolations are shown.

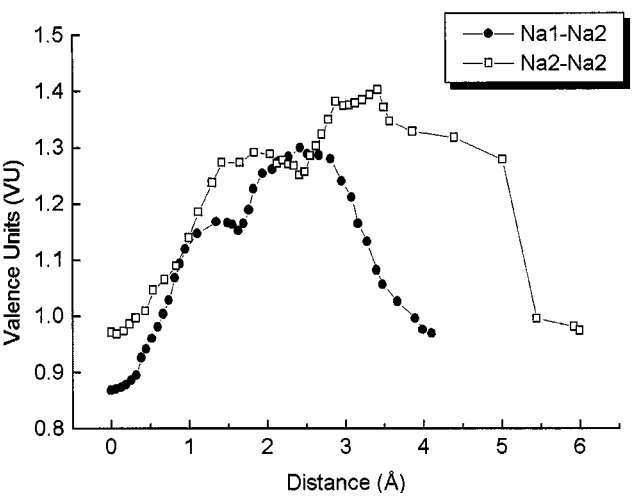

FIG. 8. $m(d)$ curves for Na1–Na2 and Na2–Na2 conduction paths for $Na_{1.5}Zr_{1.5}In_{0.5}P_3O_{12}$.

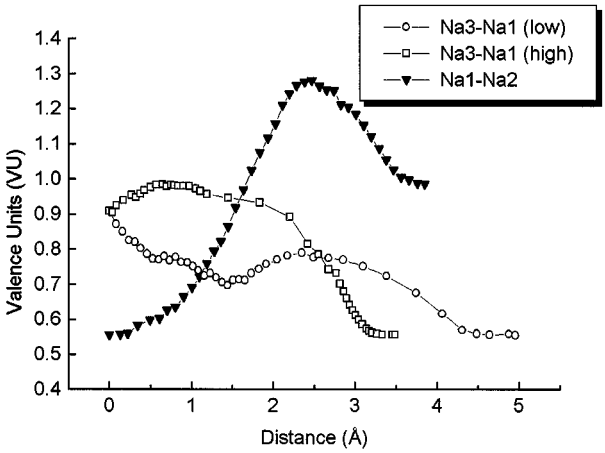

FIG. 9. $m(d)$ curves for different conduction paths in monoclinic $Na_3Zr_2Si_2PO_{12}$.

results are peculiar to the above series and are not directly extensible to other Nasicons.

Monoclinic Nasicon $Na_{(1+x)}Zr_2Si_{(x)}P_{(3-x)}O_{12}$ (with $x = 2.05$)

In the monoclinic Nasicons (s.g., $C2/c$) the Na2 position of the rhombohedral structure is splitted into two positions, Na2 and Na3 (17). According to Boilot *et al.* (9), the Na2 position is fully occupied while the Na3 site is nearly half empty and strongly displaced along the conduction channel toward the Na1 position. The monoclinic unit cell contains four Na2 positions, which are completely occupied. Na1($4\times$) and Na3($8\times$) positions are only partial occupied (3). It has been already noted (3) that the fully occupation of the Na2 position tends to inhibit ionic movement. The full occupancy of Na2 position is confirmed by its valence sum near to 1 (0.972 VU). Na1 is strongly underbonded (0.556 VU), while the Na3 position has an intermediate value of 0.890. The difficulty in Na1–Na2 movement is fully confirmed by valence analysis which yields a VUmax of 1.28 along this path. In the monoclinic structure there are, however, two nonequivalent Na1–Na3 paths, both of them having much lower valence values. The first of these two paths has a VUmax of 0.984, the second displays a very broad relative maximum, lower than the starting value of 0.984. The $m(d)$ function in this case smoothly decreases from 0.890 to 0.556 VU. As a consequence, along both Na1–Na3 paths, Na^+ ions move without reaching at any point a valence sum higher or equal to 1, as shown in Fig. 9, a fact that can explain the exceptionally high conduction of the monoclinic material. The connectivity along the network is preserved, by the fact that between two Na1 positions two channels (Na1–Na3–Na1) are active and the third (Na1–Na2–Na1) is not, as depicted in Fig. 10.

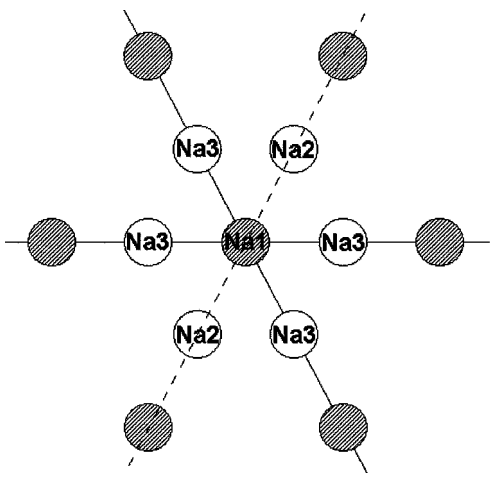

FIG. 10. Projection onto the *ab* plane of conduction connectivity for monoclinic Nasicon. Na1–Na2–Na1 path results inhibited, while Na1–Na3–Na1 are strongly enhanced.

CONCLUSIONS

Valence bond analysis has been successfully applied to model ionic pathways and conductivity in different Nasicon structures. The description of the Nasicon archetype allows us to show that rotation angles ε and ϕ of O(1), O(2) triangles from ideal positions are the main geometrical feature influencing Na^+ mobility in rhombohedral Nasicons of the series $Na_{(1+x)}Zr_2Si_{(x)}P_{(3-x)}O_{12}$ ($0 \le x \le 3$). For this Nasicon family as well as for miscellaneous Nasicons with rhombohedral symmetry the calculated ionic trajectories and the VUmax values well compare with resistivities and activation energies for ionic conduction which have been experimentally found for the same phases.

The exceptionally high ionic conductivity for monoclinic Nasicon $Na_{(1+x)}Zr_2Si_{(x)}P_{(3-x)}O_{12}$ ($2 \le x \le 2.25$) has been explained by Na1–Na3 paths, where Na^+ ions move without reaching at any point a valence sum higher or equal to 1. The connectivity along the network is preserved by the fact that between two Na1 positions two channels (Na1–Na3–Na1) are active and the third (Na1–Na2–Na1) is inactive.

REFERENCES

1. H. Y.-P. Hong, *Mater. Res. Bull.* **11,** 173–182 (1976).
2. J. B. Goodenough, H. Y.-P. Hong, and J. A. Kafalas, *Mater. Res. Bull.* **11,** 203–212 (1976).
3. W. H. Baur, J. R. Dygas, D. H. Whitmore, and J. Faber, *Solid State Ionics* **18/19,** 935–943 (1986).
4. M. Lucco-Borlera, D. Mazza, L. Montanaro, A. Negro, and S. Ronchetti, *Powder Diffr.* **12**(3), 171–174 (1997).
5. O. Bohnke, S. Ronchetti, and D. Mazza, *Solid State Ionics* **122,** 127–136 (1999).

6. H. Kohler, H. Schulz, and O. Melnikov, *Mater Res. Bull.* **18,** 1143–1152 (1983).
7. J. P. Boilot, G. Collin, and Ph. Colomban, *J. Solid State Chem.* **73,** 160–171 (1988).
8. D. TanQui, J. J. Capponi, M. Gondrand, M. Saib, J. C. Joubert, and R. D. Shannon, *Solid State Ionics* **3**/**4,** 219–222 (1981).
9. J. P. Boilot, G. Collin, and Ph. Colomban, *Mater. Res. Bull.* **22,** 669–676 (1987).
10. M. A. Subramanian, P. R. Rudolf, and A. Clearfield, *J. Solid State Chem.* **60,** 172–181 (1985).
11. E. R. Losilla, M. A. G. Aranda, S. Bruque, M. A. Paris, J. Sanz, and A. R. West, *Chem. Mater.* **10,** 665–673 (1998).
12. I. D. Brown and D. Altermatt, *Acta Crystallogr. B* **41,** 244–247 (1985).
13. I. D. Brown, *Phys. Chem. Miner.* **15,** 30–34 (1987).
14. I. D. Brown, *Z. Kristallogr.* **199,** 255–272 (1992).
15. K. Waltersson, *Acta Crystallogr. A* **34,** 901–905 (1978).
16. N. E. Brese and M. O'Keeffe, *Acta Crystallogr. B* **47,** 192–197 (1991).
17. P. R. Rudolf, M. A. Subramanian, A. Clearfiels, and J. D. Jorgensen, *Mater Res. Bull.* **20,** 643–651 (1985).